 doi:10.20944/preprints202206.0098.v1

Preclinical immunogenicity and efficacy of a multiple antigen-presenting system (MAPS™) SARS CoV-2 vaccine

Brian Cieslewicz[1], Daniel Makrinos[1,*], Heidi Burke[1], Dara Bree[1], Ranuka Haridas[1], Ian Tonkiss[1], Yannic Bartsch [2], Galit Alter [2], Richard Malley[1,4], and Gilles Besin[1#]

[1] Affinivax, Cambridge, MA 02142

[2] Ragon Institute of MGH, MIT, and Harvard, Cambridge, MA, USA.

[3] Division of Infectious Diseases, Department of Medicine, Boston Children's Hospital, Boston, MA 02115, USA.

* Current affiliation, Moderna Tx, Cambridge, MA 02139

[#] Corresponding author: gilles.besin@affinivax.com

 doi:10.20944/preprints202206.0098.v1

Abstract

Despite the remarkable success of SARS CoV-2 vaccines, the rise of variants, some of which are more resistant to the effects of vaccination, highlights the potential need for additional COVID-19 vaccines. We used the Multiple Antigen Presenting System (MAPS) technology, in which proteins are presented on a polysaccharide polymer to induce antibody, Th1, Th17 and CD8+ T cell responses, to engineer a novel vaccine targeting SARS CoV-2. This vaccine contains a fragment of the spike (S) protein receptor-binding domain (RBD) sequence of the original D614G strain and was used to immunize nonhuman primates (NHP) for assessment of immunological responses and protection against SARS CoV-2 challenge. The SARS CoV-2 MAPS vaccine generated robust neutralizing antibodies as well as Th1, Th17 and cytotoxic CD8 T-cell responses in NHPs. Furthermore, MAPS-immunized NHPs had significantly lower viral loads in the nasopharynx and lung compared to control animals. Taken together, these findings support the use of the MAPS platform to make a SARS CoV-2 vaccine. The nature of the platform also could enable its use for the inclusion of different variants in a single vaccine.

Preprints (www.preprints.org) | NOT PEER-REVIEWED | Posted: 7 June 2022 doi:10.20944/preprints202206.0098.v1

Introduction

In December 2019, a novel coronavirus was identified following a respiratory disease outbreak in Wuhan, China. This virus, designated Severe Acute Respiratory Syndrome Coronavirus 2 (SARS CoV-2), causes respiratory disease and other systemic symptoms in humans, defined as coronavirus disease 2019 (COVID-19). Several COVID-19 vaccines have been either authorized or approved, at unprecedented speed, resulting in rapid and high vaccine coverage in several countries. However, despite these impressive achievements, there are increasingly worrisome signs that vaccine-induced immunity may be short-lived, with a rise of breakthrough infections stemming from new variants of SARS CoV-2 [1]. As a result, it has become doubtful that these first-generation vaccines will provide sufficient control of the virus worldwide.

While several vaccine platforms have been used (Pfizer [2,3], Moderna[4], J&J [5], Novavax [6,7]), the most successful strategies to date involved mRNA- or DNA-based vaccines. These vaccines generate robust, neutralizing antibodies directed against the S protein of SARS CoV-2. Questions about durability and breadth of immune responses remain, particularly given growing evidence to support a role of T cells in protection [8].

In the present study, we make use of a novel vaccine platform, the Multiple Antigen Presenting System (MAPS) [9] which can induce robust antibody and T-cell responses. MAPS combines pathogen-specific proteins fused to rhizavidin (an avidin-like protein) with biotinylated polysaccharides, resulting in the formation of a complex that can elicit antibodies to all components, and T-cell responses to proteins [10]. AFX3772, a multivalent vaccine consisting of 24 pneumococcal polysaccharides and a fusion protein comprising two pneumococcal proteins and rhizavidin, has been shown to be safe and immunogenic in healthy adult and older adults [11]. Here the RBD of the original SARS CoV-2 strain (D614G) was genetically fused to rhizavidin and

Preprints (www.preprints.org) | NOT PEER-REVIEWED | Posted: 7 June 2022 doi:10.20944/preprints202206.0098.v1

purified from eukaryotic cells. This fusion protein was then combined with a biotinylated polysaccharide (type 1 from *Streptococcus pneumoniae*) to form a MAPS complexes [12,13] (see Figure 1B). This SARS CoV-2 MAPS vaccine was then tested in rabbits and in non-human primates (NHP) for evaluation of immunogenicity and protection against viral challenge.

Preprints (www.preprints.org) | NOT PEER-REVIEWED | Posted: 7 June 2022 doi:10.20944/preprints202206.0098.v1

RESULTS

Manufacture of SARS CoV-2 MAPS

Expression of S-RBD-Rhizavidin fusion protein in eukaryotic cells: The fusion protein S-RBD-Rhizavidin was obtained by fusing the S-RBD sequences (fragment corresponding to AA 331- 524) to the gene sequence encoding the rhizavidin (fragment corresponding to AA 45-179) and cloned into pFastBac1 plasmid; the baculovirus expression system was used to express the fusion construct in SF900II cells. This His-tagged recombinant protein was then purified using nickel-nitrilotriacetic acid (NTA) affinity chromatography and was analyzed using SDS-PAGE **(Fig 1A)**. The rhizavidin dimer is very stable and remains intact in reducing SDS buffer, maintaining its ability to bind biotin-4-fluorescein (B4F), and dissociates only after heating to 100°C in reducing SDS [14].

Human Angiotensin Converting Enzyme 2 (hACE2) receptor binding assay: To demonstrate the preservation of the relevant S-RBD protein epitopes, we performed an hACE2 receptor binding assay. The data demonstrated strong binding of the S-RBD-Rhizavidin fusion protein to the hACE2 receptor in a concentration-dependent matter, thus indicating that the RBD protein in the fusion remained functional **(Fig 1C).**

MAPS formation. MAPS complex was assembled by incubation of biotinylated polysaccharide with the fusion protein at 4°C overnight then purified via preparative size exclusion chromatography. Purified MAPS and components were examined by HPLC-SEC (**Fig 1D**), larger molecules of MAPS and polysaccharide eluted at the void volume of t=+/-12 minutes while unlinked protein antigens are retained longer and elute later from the column (t=+/-21 minutes). Molecular weights of the complexes were compared using multi-angle light scattering (MALS),

Preprints (www.preprints.org) | NOT PEER-REVIEWED | Posted: 7 June 2022 doi:10.20944/preprints202206.0098.v1

showing that MAPS complexes had a weight average molecular weight of 4256 kDa, polysaccharide 768 kDa, and S-RBD-Rhizavidin dimer of 79.1 kDa in figure (**Fig 1E**).

As shown previously [14], the association between polysaccharide and protein antigens in MAPS is very stable, resistant to treatment with reducing SDS buffer, and undergoes dissociation only upon heating to 100°C in SDS, allowing for estimation of assembly efficiency by comparing the SDS-PAGE antigen profiles of unheated and heated samples [14]. The incorporation of S-RBD-Rhizavidin fusion protein into MAPS complexes was confirmed by SDS-PAGE of the purified MAPS complex (MAPS non-heated and heated sample lanes) **(Fig 1F)**. In the heated samples there is a band corresponding to the monomer of the target antigen whereas in the non-heated MAPS sample, the fusion protein does not migrate as it is retained with the affinity-linked polysaccharide in the well.

Immunogenicity of the SARS CoV-2 MAPS in rabbits

New Zealand rabbits (n=3) were immunized with 2 subcutaneous inoculations of SARS CoV-2 S-RBD MAPS vaccine at Day 0 and 21 (**Fig 2A**). The antibody responses against SARS CoV-2 S protein were measured on Day 0 (baseline before injection, P0), Day 21 (representing the response after the first immunization, P1), and again on Day 42 (representing the response after the second immunization, P2) by ELISA and virus neutralization assay (VNT). We noted an increase in serum concentration of antibodies to S and neutralizing antibody activity, especially after the second dose (**Fig 2B and C**).

Immunogenicity of the SARS CoV-2 MAPS vaccine in Cynomolgus macaques

Adult Cynomolgus macaques (n=6, males, 3.3–5.0 years-old) were immunized with 2 subcutaneous inoculations of SARS CoV-2 MAPS vaccine at Day 0 and 21 (**Fig 3A**). An aged-matched control group (n= 6, males, 3.3–5.0 years-old) received an injection of saline at Day 0

Preprints (www.preprints.org) | NOT PEER-REVIEWED | Posted: 7 June 2022 doi:10.20944/preprints202206.0098.v1

and 21. SARS CoV-2 S–specific antibody responses were measured 21 days post first injection, before the second injection (P1) and again 21 days post second injection (P2) by ELISA and virus neutralization assay (VNT). **Fig 3B** shows the increase in antibodies to S after the first and second immunizations. The concentration of RBD-specific subclass IgG was measured by Luminex based assay: IgG1 (**Fig 3C**). and IgG3 (**Fig 3D**) antibodies directed against S and S1 domain were detected, but this was not the case for the S2 domain, which is not included in the vaccine. The specificity of the measured response was further confirmed by the absence of ELISA signal to SARS CoV-2 nucleoprotein (N) and the influenza HA protein.Similar to the IgG responses in ELISA, we detected neutralizing antibody responses at Day 21 (**Fig 3E**) which increased even further after the second immunization (**Fig 3E**).

To evaluate for the presence of cross-reactive antibodies against variant strains, we compared the concentration of antibodies directed against the RBD sequence of the D614G, alpha (B1.1.7), or gamma (B1.351) variant in NHP sera following immunization with SARS CoV-2 MAPS. In the same experiment, sera from patients who recovered from COVID-19 were also included, to evaluate the presence of cross-reactive antibodies in human **(Fig 3F)**. The concentration of total IgG directed against S-RBD was highest against the RBD derived from the D614G strain compared to that directed against either of the two variants. We observed similar results from immunized animals and from human convalescent sera.

Evaluation of the effector function of SARS CoV-2 MAPS-induced antibodies

Opsonophagocytic and cytotoxic function depend on the ability of antibodies to interact with Fc-receptors found on immune cells [15]. In humans and nonhuman primates, four low affinity Fc-receptors (FcγR2a, FcγR2b, FcγR3a, and FcγR3b) drive IgG-mediated activation [16].

Preprints (www.preprints.org) | NOT PEER-REVIEWED | Posted: 7 June 2022 doi:10.20944/preprints202206.0098.v1

To evaluate the Fc effector function of antibodies generated following two immunizations with SARS CoV-2 MAPS, we used a systems serology approach published previously [17] to evaluate antibody-dependent cellular phagocytosis (ADCP), antibody-dependent neutrophil phagocytosis (ADNP), and antibody-dependent complement deposition (ADCD). When compared to sera from NHPs that had received saline alone, sera from NHPs immunized with SARS CoV-2 MAPS bound more to FcγR2a (**Fig 4A**) and FcγR2b (**Fig 4B**) in the presence of S, S1 or S-RBD protein. No increase in binding was observed in the presence of control proteins S2, or N SARS CoV-2, or HA.

Finally, to explore the functional impact of vaccine-induced antibody Fc-profiles, we examined cellular monocyte phagocytosis (ADCP, **Fig 4C**), neutrophil phagocytosis (ADNP, **Fig 4D**), and complement deposition (ADCD, **Fig 4E**). All these effector functions were observed in sera obtained from SARS CoV-2-immunized NHP in the presence of the S protein; as expected, none of these activities was seen in the presence of the N protein.

SARS CoV-2 MAPS vaccine drives a potent cellular immune response in cynomolgus macaques

S-RBD-specific T-cell responses were analyzed in vaccinated and placebo NHP groups by intracellular cytokine staining (ICS). The SARSCoV-2 MAPS vaccine generated significantly increased S-RBD-specific IFN-γ-producing T-cell responses, including higher frequencies of CD4+ Th1 cells (**Fig 5A**), CD8+ T cells (**Fig 5D**), and TNFα-producing CD8+ T-cells (**Fig 5E**). Both Th1 and Th17 cell frequency (**Fig 5C**) were also increased in vaccinated NHPs compared to the placebo group. Finally, significantly greater numbers of IL-4 producing CD4+ T-cells (**Fig 5B**) were detected in SARS CoV-2 MAPS vaccinated NHPs compared to placebo vaccinated NHPs.

Protective efficacy against upper and lower-airway SARS CoV-2 infection

Preprints (www.preprints.org) | NOT PEER-REVIEWED | Posted: 7 June 2022 doi:10.20944/preprints202206.0098.v1

All animals were challenged by combined intratracheal and intranasal routes as previously described [18], with a total dose of 10^5 PFU of the D614G strain of SARS CoV-2 administered 4 weeks after the second vaccination. Due to the importance of nasal epithelial and pulmonary cells in SARS CoV-2 infection [19–21], both nasal washes and bronchoalveolar lavage (BAL) samples were tested for SARS CoV-2 RNA by reverse-transcription quantitative polymerase chain reaction (RT-qPCR) or Median Tissue Culture Infectious Dose ($TCID_{50}$) assays **(Fig. 6)**. In NHPs that received saline alone, viral RNA was detected in nasal swabs obtained from Day 1 to Day 8 after challenge, both by RT-qPCR (**Fig. 6A)** and $TCID_{50}$ (**Fig. 6B)**. In vaccinated NHPs, viral RNA was detected in 2/6 nasal swab by RT-qPCR; by Day 4, all nasal swabs were negative (**Fig. 6A).** By $TCID_{50}$, 4/6 NHP were positive on Day 1 but quickly reverted to negative (**Fig. 5B)**. From BAL samples, viral RNA was detected in 3 of 6 unimmunized NHPs on Days 2 and 4 after challenge (**Fig. 6 C and D**) whereas viral RNA was detected in the BAL of only 1 of 6 immunized NHP at Day 2 and no viral RNA was detected at later timepoints.

Of interest, we observed an increase of the antibody response after the challenge in the vaccinated NHPs (including one animal that had no detectable neutralization antibody after dose 2 and prior to challenge) whereas no neutralizing antibody was detected in the unimmunized NHPs (**Fig 3E**), suggesting a boosting effect following exposure to the virus.

Preprints (www.preprints.org) | NOT PEER-REVIEWED | Posted: 7 June 2022 doi:10.20944/preprints202206.0098.v1

DISCUSSION

In response to the COVID-19 pandemic, the scientific and biopharmaceutical community has rallied with unprecedented speed to develop effective vaccines to combat this novel pathogen. Many vaccine platforms have been utilized to develop a COVID-19 vaccine quickly, with several already approved for human use barely within a year of the emergence of the virus. Despite this remarkable success, the rise of SARS CoV-2 variants, some of which are more resistant to the effects of vaccination, highlights the potential need for additional COVID vaccines. In comparison to DNA- or RNA- based vaccines, protein-based vaccines may be associated with fewer side effects, but are not yet in widespread use for COVID-19, even though late-stage clinical-trial data looks promising. In this manuscript, we describe the use of the MAPS vaccine platform , which relies on an affinity-based association between polysaccharides and proteins to elicit immune response against bacterial and viral targets. The findings reported here demonstrate that two doses of this prototype SARS CoV-2 MAPS in a NHP model. Importantly, the neutralizing antibody responses observed before challenge in vaccinated animals were comparable to those measured in prior studies using similar assays following 100μg of the mRNA-based vaccines, mRNA1273 [22] and BNT162b [2] and higher than those measured in convalescent humans.

We also show that immunization with MAPS generates both CD4+ and CD8+ T cells directed against the SARS-CoV-2 RBD. The importance of T cells in disease severity and duration and driving recovery from SARS CoV- 2 infection has been shown in animal and human studies. Notably studies in non-human primates demonstrated that SARS-CoV-2-specific T cells offer a substantial level of protection from SARS CoV-2 infection and improved outcome [23]. Similarly T-cell-mediated protection from coronaviruses, including SARS CoV-2, in mice has been reported [24,25]. Clincially early induction of interferon (IFN)-γ-secreting SARS CoV-2-specific T cells

Preprints (www.preprints.org) | NOT PEER-REVIEWED | Posted: 7 June 2022 doi:10.20944/preprints202206.0098.v1

was associated with milder disease in COVID-19 patients [26]. In another study, lower disease severity was associated with increased SARS-CoV-2-specific CD8+ and CD4+ T cells ([27] T cell responses have been documented in humans following vaccination with either adenoviral vectors (25) or mRNA-based vaccines (26). We show here that the SARS CoV-2 MAPS vaccine elicited both IFN-γ secreting $CD4^+$ and IFN-γ secreting $CD8^+$ in NHP. While the optimal T cell profile remain to be determined, it is important to note that the vaccine studied here generated a balanced Th1, Th2 and Th17 $CD4^+$ T cell response.

Furthermore, we demonstrate that SARS CoV-2 MAPS vaccine was able to inhibit viral replication in both the upper and lower airways (BAL) by day 2 for most of the animals (5 out of 6), with no detectable virus in all animals by day 4. We observed a complete reduction in viral titers at day 2 for most of the animals (5 out of 6), with no detectable virus in all animals in the by day 4, comparable to what was observed in NHP challenge model with other vaccines using a challenge dose similar to the one used here [22,28].

Among the currently authorized COVID-19 vaccines, the two mRNA vaccines (BNT162b2 and mRNA-1273) have been the most widely used for both primary series and boosting. However, heterologous boosting, such as combining mRNA vaccines with adenovirus-vectored vaccines, has been shown to be advantageous in humans, leading to higher S-specific IgG, neutralizing antibodies, and S-specific $CD4^+$ T cells than after homologous boosting [29–31]. Although mRNA vaccines are currently being used as boosters, other options, such as protein-based vaccines, could become more attractive, for tolerability and/or immunogenicity reasons.

In summary, we demonstrate here the potential of the MAPS platform to induce neutralizing antibody and T-cell responses directed against the S-RBD. As previously demonstrated in the context of *S. pneumonias and S. aureus* [9,12], the MAPS platform allows for the inclusion of

 doi:10.20944/preprints202206.0098.v1

multiple protein antigens in the same construct. This approach may be particularly attractive in the context of COVID-19 vaccines as incorporating multiple RBD variants could provide a powerful tool to combat emerging variants.

Preprints (www.preprints.org) | NOT PEER-REVIEWED | Posted: 7 June 2022 doi:10.20944/preprints202206.0098.v1

MATERIALS AND METHODS

Construction, expression, and purification of S-RBD-Rhizavidin fusion antigens.

The fusion protein S-RBD-Rhizavidin was obtained by fusing the S-RBD sequence (fragment corresponding to AA 331- 524) to the gene sequence encoding the rhizavidin (Rhizavidin) fragment as previously described [14] The fusion construct was cloned into the pFastBac1 plasmid and transfected into SF900II cells for expression. His-tagged recombinant proteins were purified using nickel-nitrilotriacetic acid (NTA) affinity chromatography. To improve purity, the eluents of the affinity column were then subjected to SEC on a Superdex 200 column. The peak fractions containing the fusion proteins were collected, evaluated by SDS/PAGE, and then flash-frozen in liquid nitrogen for future use. Protein concentration was measured using a bicinchoninic acid (BCA) protein assay kit (Pierce).

Manufacture of SARS CoV-2 MAPS

Each MAPS complex was assembled by incubation of biotinylated polysaccharide with fusion antigens at 4°C overnight. The assembled complex was isolated by SEC, using Tris-buffered saline (20 mM Tris-HCl pH 8.0, 150 mM NaCl) as an eluant. The fractions containing MAPS complex were pooled. The protein concentration in a MAPS complex was measured using a bicinchoninic acid (BCA) protein assay kit (Pierce), and the polysaccharide concentration was determined by uronic acid assay.

Evaluation of SARS CoV-2 MAPS vaccine by Analytical HPLC-SEC-MALS

Samples were analyzed via HPLC-SEC. Approximately 20 micrograms of each sample were injected onto an AdvanceBio SEC 1.9 μm column (Agilent) on Waters Acquity HPLC. Samples were flowed over the column at 0.4 ml/minute in 20 mM HEPES, 100 mM sodium chloride at 25°C maintaining pre-column pressure of approximately 1500 PSI. In line detectors measured UV

Preprints (www.preprints.org) | NOT PEER-REVIEWED | Posted: 7 June 2022 doi:10.20944/preprints202206.0098.v1

absorbance at 280nm following the column. Absorbances were normalized to the maximum absorbance within each run and plotted against one another. MALS data were generated using Wyatt Dawn and Wyatt Optilab differential refractometer. Samples were gated at full width at half maximum while using a first order Zimm fit to generate molecular weight data.

Evaluation of S-RBD-Rhizavidin protein and SARS CoV-2 MAPS vaccine by SDS-PAGE

Samples were diluted with water and reducing Laemmli buffer. Additionally, biotin-4-fluorescein (B4F) (Invitrogen, CA) was added to the protein purification samples at a final concentration of 2 mg/ml. Samples were then either incubated at room temperature (RT) or heated at 100°C for ten minutes. One microgram of each sample was loaded on a 4-12% Bis-Tris Protein gel (Invitrogen) and then ran for 40 minutes at 200 volts. The gel was then stained with InstantBlue Coomassie Protein Stain (Abcam) for 15 minutes and rinsed with water. The gel was exposed for 0.5 seconds on the Bio-Rad ChemiDocMP imager.

Determination of S-RBD-Rhizavidin binding to hACE2 receptor

Plates were precoated with hACE2 receptor overnight and washed with phosphate-buffered saline with 0.05% Tween (PBS-T) buffer and blocked with TBS Startblock blocking buffer (Thermo Fisher Scientific, PA). Histidine-tagged S-RBD-Rhizavidin was threefold serially diluted and added to coated wells for 2 hours at RT. Following washing, 100 µl of anti His-HRP (Bio-Rad, CA) was added to the plate. Plates were incubated for 1 hour at RT, while SureBlue TMB Microwell Peroxidase Substrate (VWR, PA) equilibrated to RT. After a final wash, 100 µl TMB substrate was added to wells and development was stopped with 100 µl of 1N hydrochloric acid after 10 minutes at RT. The ELISA plates were read at an absorbance of 450 nm on a SpectraMax i3x Plate Reader using Softmax Pro 7.0.

Rabbit immunization

Preprints (www.preprints.org) | NOT PEER-REVIEWED | Posted: 7 June 2022 doi:10.20944/preprints202206.0098.v1

All rabbit immunizations were performed at Cocalico Biologics (Stevens, PA). Female New Zealand White rabbits (n=3/ group) were injected intramuscularly (IM) with either 50 µg of SARS CoV-2 MAPS vaccine or saline vehicle (0.5 ml). Booster injections were given at Day 21 and Day 42 post-first injection. Sera were obtained before each immunization and at a terminal bleed on Day 56 for measurement of antibodies. Observations for morbidity, mortality, clinical signs, body temperature, food and water consumption were conducted on a regular basis for all animals.

Non-human primate immunization and challenge.

The study was performed by BIOQUAL, Inc. (Rockville MD). The study was conducted in accordance with the Study Protocol and BIOQUAL Standard Operating Procedures (SOPs) when applicable, and in accordance with the animal welfare requirements and accreditations stated below. The study was performed in compliance with the following regulations or guidelines: Housing and handling of the animals were performed in accordance with the standards of the AAALAC lnternational's reference resource: the 8th edition of the Guide for the Care and Use of Laboratory animals, Animal Welfare Act as amended, and the 2015 reprint of the Public Health Service (PHS) Policy on Human Care and Use of Laboratory Animals. Handling of samples and animals occurred in compliance with the Biosafety in Microbiological and Biomedical Laboratories (BMBL), 5th edition (Centers for Disease Control). This study was performed under IACUC protocol #20-113. Approved on September 15th, 2020.

A total of 12 adult male, cynomolgus macaques (Mauritian origin, Macaca fascicularis), about 3-4 kg at time of delivery, were purchased from PreLabs (Lehigh Acres, FL). In vivo procedures were performed according to the approved animal protocols at Bioqual Inc. All components of the study were conducted at Bioqual Inc (Baltimore, MD) except for the intracellular cytokine staining which was conducted at Affinivax.

Preprints (www.preprints.org) | NOT PEER-REVIEWED | Posted: 7 June 2022 doi:10.20944/preprints202206.0098.v1

The animals (n=6/group) were injected subcutaneously (SQ) with either 100 µg of SARS CoV-2 MAPS vaccine or saline vehicle (1 ml). A booster injection was given at Day 21 post-first injection. Sera were collected prior to and following each immunization to evaluate induction of antibody responses and cellular immunity to the vaccine antigen. Blood was collected to isolate PBMCs at Day 42 from animals immediately prior to challenge with 10^5 PFU/2ml of SARS CoV-2 USA-WA1/2020 isolate via the combination intranasal/intratracheal (IN/IT) route. Nasal swabs and BAL were collected throughout the post challenge phase to monitor viral load over time. Animals were monitored for symptoms through post-challenge from Days 42-56 followed by euthanasia for necropsy and tissue collection.

Isolation of peripheral blood mononuclear cells (PBMCs)

CPT tubes were spun as follows for isolation of PBMCs: 2,700 rpm for 30 minutes followed by 3 spins/washes at 1,500, 1,200, and 1,000 rpm each for 10 minutes. The live vs. dead PBMCs were enumerated using a Nexcelom Cellometer K2 (SOP# BV-031). The PBMCs were then resuspended in FBS with 10% DMSO using Mr. Frosty® (Thermo Scientific, PA) or similar freezing boxes. The boxes were placed immediately into a -80°C freezer for 24 hours and then transferred for storage in a liquid nitrogen tank. The number of cells per vial is typically 5-10 million and viability is normally >90%.

SARS CoV-2 S, S subunit, RBD, and N IgG ELISA

Sandwich ELISA was performed to quantify serum IgG levels (Rauch et al 2020). Nunc-Immuno MaxiSorp 96-well plates were coated with 4 µg/ml of SARS CoV-2 S-RBD, his-tag (Wild-Type, SPD-C52H3, Acro biosystems, DE), SARS CoV-2 S-RBD (N501Y), his-tag (UK Mutant, SPD-C52Hn, Acro biosystems, DE), S-P2 Spike,his-tag (Trimer, UWashington, 35962), RBD Soluble, his-tag (UWashington, 35961), and SARS-CoV-1 (S1 Subunit) S-RBD (40150-V08B1, Sino

Preprints (www.preprints.org) | NOT PEER-REVIEWED | Posted: 7 June 2022 doi:10.20944/preprints202206.0098.v1

biologicals, PA) and left overnight at RT. Similarly, AffiniPure F(ab')2 Fragment-specific goat anti-human IgG (Jackson Laboratory, ME) was coated for standards. IgG ELISA plates were washed (BioTek 405 TS) in 1x DPBS-T (0.05% Tween-20) and blocked with 1% bovine serum albumin (BSA) (Millipore Sigma, MA) for 1 hour at RT. After blocking, plates were washed and 100 µL of diluted sera/ purified human IgG (MP Biomedicals, CA) were added to the antigen-coated plate and incubated for 1 hour at RT. Following washing, a Goat Anti-Human (H+L)-HRP (Bio-Rad, CA) was diluted to 1:20,000 in 1x DPBS-T and added 100 µL/well to the plate. Plates were incubated for 1 hour at RT, while SureBlue TMB Microwell Peroxidase Substrate (VWR, PA) equilibrated to RT. After a final wash, 100 µL TMB substrate was added to wells and development was stopped with 100 µL of 1N hydrochloric acid after 10 minutes at RT. The ELISA plates were read at an absorbance of 450 nm on a SpectraMax i3x Plate Reader using Softmax Pro 7.0.

Plaque reduction neutralization test (PRNT)

SARS CoV-2 neutralization was assessed as previously described [32]. In brief, a pre-titrated dose of virus was incubated with 8 serial 5-fold dilutions of serum samples in duplicate in a total volume of 150 µL for 1 hour at 37°C in 96-well flat-bottom poly-L-lysine-coated Biocoat plates (catalog number 354461, Corning, NY, USA). Cells were suspended using TrypLE Select Enzyme solution (Thermo Fisher Scientific, PA) and immediately added to all wells (10,000 cells in 100 µL of growth medium per well). One set of 8 control wells received cells +virus (virus control) and another set of 8 wells received cells only (background control). After 66-72 hours of incubation, medium was removed by gentle aspiration and 30 µL of Promega 1X lysis buffer was added to all wells. After a 10-minute incubation at RT, 100 µL of Bright-Glo luciferase reagent was added to all wells. After 1-2 minutes, 110 µL of the cell lysate was transferred to a black/white plate (Perkin-

Preprints (www.preprints.org) | NOT PEER-REVIEWED | Posted: 7 June 2022 doi:10.20944/preprints202206.0098.v1

Elmer). Luminescence was measured using a PerkinElmer Life Sciences, Model Victor2 luminometer. Neutralization titers are the serum dilution at which relative luminescence units (RLU) were reduced by 50% (ID_{50}) compared to virus control wells after subtraction of background RLUs. Serum samples were heat-inactivated for 30 minutes at 56°C prior to the assay.

Antibody-dependent complement deposition

Antibody-dependent complement deposition (ADCD) was assessed as described previously [33]. In brief, biotinylated antigen was coupled to fluorescent NeutrAvidin beads (Thermo Fisher Scientific, PA). Plasma antibodies were diluted 1:10 in 0.1% BSA and incubated with the coupled antigen beads for 2 hours at 37 °C. Beads were washed and incubated with complement factors from guinea pig for 20 min at 37 °C. The complement reaction was then stopped by washing with 15 mM EDTA in PBS. C3 deposition on the beads was detected with a 1:100 diluted FITC-conjugated anti-guinea pig C3 polyclonal antibody (MP Biomedicals), and relative C3 deposition was analyzed by flow cytometry.

Antibody-dependent neutrophil phagocytosis

Antibody-dependent neutrophil phagocytosis (ADNP) was assessed as described previously [34]. Briefly, primary human neutrophils were obtained from ACK lysed blood of healthy donors.Biotinylated antigens were incubated with NeutrAvidin beads and ICs formed by incubation with 1:100 diluted plasma for 2 hours at 37 °C in 96-well plates (Greiner Bio-One). Isolated neutrophils were added afterwards and incubated for 1 hours at 37 °C. Neutrophils were surface stained against CD66b (1:50, Biolegend, clone: G10F5), fixed with 4% paraformaldehyde and analyzed on an LSRII (BD) flow cytometer. Phagocytosis score was calculated as the product of frequency beads positive CD66b neutrophils and bead fluorescent intensity using FlowJo 10.8.

Antibody-dependent cellular phagocytosis

Preprints (www.preprints.org) | NOT PEER-REVIEWED | Posted: 7 June 2022 doi:10.20944/preprints202206.0098.v1

Antibody-dependent cellular phagocytosis (ADCP) was assessed as described previously [35]. In brief, THP-1 monocyte phagocytosis was performed as previously described. Briefly, biotinylated antigens were conjugated to NeutrAvidin beads and incubated with 1:100 diluted plasma samples. THP-1 monocytes (0.25 million cells per well) were added to the ICs and incubated for 16 hours at 37 °C, fixed with 4% paraformaldehyde and analyzed by flow cytometry.

IgG Subclass, isotype and FcR-binding Luminex profiling

IgG subclass and FcR profiling was conducted as previously described [36],[37]. Briefly, antigens were carboxyl coupled to magnetic Luminex microplex carboxylated beads (Luminex Corporation, TX) using NHS-ester linkages with Sulfo-NHS and EDC (Thermo Fisher, PA), and then incubated with serum for 2 hours at room temperature. Subclass (IgG1 or IgG3) titer were first probed with a mouse rhesus-subclass IgG1 or IgG3 specific secondary antibody (NHP Reagent Resource), respectively, mouse IgG was then detected with a PE-conjugated anti-mouse antibody (Thermo-Fisher). FcR binding was quantified by incubating immune complexes with biotinylated FcRs (FcγR2A-1, FcγR2A-2, FcγR3A, Duke Protein Production Facility) conjugated to Steptavidin-PE (Prozyme, CA). Flow cytometry was performed with an IQue (Intellicyt, NM), and analysis was performed on IntelliCyt ForeCyt (v8.1).

Subgenomic mRNA assay

Replicating virus load by qRT-PCR targeting the subgenomic envelope (E) gene RNA in 250 ml aliquot of nasopharyngeal swabs, nasal washes, and BAL aspirates. The forward and reverse primers, probe used here were:

SUBGEN-FORWARD: 5'-CGATCTCTTGTAGATCTGTTCTC-3'

E_Sarbeco_R2 Reverse rimer: 5'-ATATTGCAGCAGTACGCACACA-3'

Probe (Thermo): FAM-MGB: 5'-ACACTAGCCATCCTTACTGCGCTTCG-3'

Preprints (www.preprints.org) | NOT PEER-REVIEWED | Posted: 7 June 2022 doi:10.20944/preprints202206.0098.v1

Infectious Viral Load ($TCID_{50}$) Assay

Vero E6 cells (ATCC no. CRL-1586) were plated at 25,000 cells/well in DMEM + 10% FBS + Gentamicin and the cultures are incubated at 37°C, 5.0% CO_2. Cells were 80-100% confluent the following day. Medium was aspirated and replaced with 180 µL of DMEM + 2% FBS + gentamicin. Twenty (20) µL of sample was added to top row in quadruplicate and mixed using a P200 pipettor 5 times. Using the pipettor, 20 µL was transferred to the next row, and repeated down the plate (columns A-H) representing 10-fold dilutions. Positive (virus stock of known infectious titer in the assay) and negative (medium only) control wells were included in each assay set-up. The plates were incubated at 37°C, 5.0% CO_2 for 4 days. The cell monolayers were visually inspected for CPE. The $TCID_{50}$ value was calculated using the Read-Muench formula.

 doi:10.20944/preprints202206.0098.v1

AUTHOR CONTRIBUTION

Conceptualization, GB and RM.; Methodology, DM, YB, BC and RH.; Writing – Original Draft Preparation, GB, RM and DB.; Writing – Review & Editing, RM, YB, GA, HB and IT.; Supervision, GB.; Project Administration, GB and IT

REFERENCES

1. Keehner, J.; Horton, L.E.; Binkin, N.J.; Laurent, L.C.; Pride, D.; Longhurst, C.A.; Abeles, S.R.; Torriani, F.J. Resurgence of SARS-CoV-2 Infection in a Highly Vaccinated Health System Workforce. *N. Engl. J. Med.* **2021**, *385*, 1330–1332, doi:10.1056/NEJMc2112981.
2. Vogel, A.B.; Kanevsky, I.; Che, Y.; Swanson, K.A.; Muik, A.; Vormehr, M.; Kranz, L.M.; Walzer, K.C.; Hein, S.; Güler, A.; et al. *A Prefusion SARS-CoV-2 Spike RNA Vaccine Is Highly Immunogenic and Prevents Lung Infection in Non-Human Primates*; Immunology, 2020;
3. Walsh, E.E.; Frenck, R.W.; Falsey, A.R.; Kitchin, N.; Absalon, J.; Gurtman, A.; Lockhart, S.; Neuzil, K.; Mulligan, M.J.; Bailey, R.; et al. Safety and Immunogenicity of Two RNA-Based Covid-19 Vaccine Candidates. *N. Engl. J. Med.* **2020**, NEJMoa2027906, doi:10.1056/NEJMoa2027906.
4. Jackson, L.A.; Anderson, E.J.; Rouphael, N.G.; Roberts, P.C.; Makhene, M.; Coler, R.N.; McCullough, M.P.; Chappell, J.D.; Denison, M.R.; Stevens, L.J.; et al. An MRNA Vaccine against SARS-CoV-2 — Preliminary Report. *N. Engl. J. Med.* **2020**, NEJMoa2022483, doi:10.1056/NEJMoa2022483.
5. Sadoff, J.; Gray, G.; Vandebosch, A.; Cárdenas, V.; Shukarev, G.; Grinsztejn, B.; Goepfert, P.A.; Truyers, C.; Fennema, H.; Spiessens, B.; et al. Safety and Efficacy of Single-Dose Ad26.COV2.S Vaccine against Covid-19. *N. Engl. J. Med.* **2021**, *384*, 2187–2201, doi:10.1056/NEJMoa2101544.
6. Dunkle, L.M.; Kotloff, K.L.; Gay, C.L.; Áñez, G.; Adelglass, J.M.; Barrat Hernández, A.Q.; Harper, W.L.; Duncanson, D.M.; McArthur, M.A.; Florescu, D.F.; et al. Efficacy and Safety of NVX-CoV2373 in Adults in the United States and Mexico. *N. Engl. J. Med.* **2022**, *386*, 531–543, doi:10.1056/NEJMoa2116185.
7. Heath, P.T.; Galiza, E.P.; Baxter, D.N.; Boffito, M.; Browne, D.; Burns, F.; Chadwick, D.R.; Clark, R.; Cosgrove, C.; Galloway, J.; et al. Safety and Efficacy of NVX-CoV2373 Covid-19 Vaccine. *N. Engl. J. Med.* **2021**, *385*, 1172–1183, doi:10.1056/NEJMoa2107659.
8. Moss, P. The T Cell Immune Response against SARS-CoV-2. *Nat. Immunol.* **2022**, *23*, 186–193, doi:10.1038/s41590-021-01122-w.
9. Zhang, F.; Lu, Y.-J.; Malley, R. Multiple Antigen-Presenting System (MAPS) to Induce Comprehensive B- and T-Cell Immunity. *Proc. Natl. Acad. Sci.* **2013**, *110*, 13564–13569, doi:10.1073/pnas.1307228110.
10. Zhang, F.; Thompson, C.; Ma, N.; Lu, Y.-J.; Malley, R. Carrier Proteins Facilitate the Generation of Antipolysaccharide Immunity via Multiple Mechanisms. *mBio* **2022**, e03790-21, doi:10.1128/mbio.03790-21.
11. Gurunadh R Chichili Safety and Immunogenicity of ASP3772, a Novel 24-Valent Pneumococcal Vaccine, in Older Adults. Presented at the ECCMID 2021.
12. Zhang, F.; Ledue, O.; Jun, M.; Goulart, C.; Malley, R.; Lu, Y.-J. Protection against *Staphylococcus Aureus* Colonization and Infection by B- and T-Cell-Mediated Mechanisms. *mBio* **2018**, *9*, e01949-18, /mbio/9/5/mBio.01949-18.atom, doi:10.1128/mBio.01949-18.
13. Choi, E.H.; Zhang, F.; Lu, Y.-J.; Malley, R. Capsular Polysaccharide (CPS) Release by Serotype 3 Pneumococcal Strains Reduces the Protective Effect of Anti-Type 3 CPS Antibodies. *Clin. Vaccine Immunol.* **2016**, *23*, 162–167, doi:10.1128/CVI.00591-15.

14. Zhang, F.; Lu, Y.-J.; Malley, R. Multiple Antigen-Presenting System (MAPS) to Induce Comprehensive B- and T-Cell Immunity. *Proc. Natl. Acad. Sci.* **2013**, *110*, 13564–13569, doi:10.1073/pnas.1307228110.
15. Bruhns, P.; Jönsson, F. Mouse and Human FcR Effector Functions. *Immunol. Rev.* **2015**, *268*, 25–51, doi:10.1111/imr.12350.
16. Hogarth, P.M.; Anania, J.C.; Wines, B.D. The FcγR of Humans and Non-Human Primates and Their Interaction with IgG: Implications for Induction of Inflammation, Resistance to Infection and the Use of Therapeutic Monoclonal Antibodies. In *Fc Receptors*; Daeron, M., Nimmerjahn, F., Eds.; Current Topics in Microbiology and Immunology; Springer International Publishing: Cham, 2014; Vol. 382, pp. 321–352 ISBN 978-3-319-07910-3.
17. Chung, A.W.; Kumar, M.P.; Arnold, K.B.; Yu, W.H.; Schoen, M.K.; Dunphy, L.J.; Suscovich, T.J.; Frahm, N.; Linde, C.; Mahan, A.E.; et al. Dissecting Polyclonal Vaccine-Induced Humoral Immunity against HIV Using Systems Serology. *Cell* **2015**, *163*, 988–998, doi:10.1016/j.cell.2015.10.027.
18. Singh, D.K.; Ganatra, S.R.; Singh, B.; Cole, J.; Alfson, K.J.; Clemmons, E.; Gazi, M.; Gonzalez, O.; Escobedo, R.; Lee, T.-H.; et al. *SARS-CoV-2 Infection Leads to Acute Infection with Dynamic Cellular and Inflammatory Flux in the Lung That Varies across Nonhuman Primate Species*; Immunology, 2020;
19. HCA Lung Biological Network; Sungnak, W.; Huang, N.; Bécavin, C.; Berg, M.; Queen, R.; Litvinukova, M.; Talavera-López, C.; Maatz, H.; Reichart, D.; et al. SARS-CoV-2 Entry Factors Are Highly Expressed in Nasal Epithelial Cells Together with Innate Immune Genes. *Nat. Med.* **2020**, *26*, 681–687, doi:10.1038/s41591-020-0868-6.
20. Ahn, J.H.; Kim, J.; Hong, S.P.; Choi, S.Y.; Yang, M.J.; Ju, Y.S.; Kim, Y.T.; Kim, H.M.; Rahman, M.T.; Chung, M.K.; et al. Nasal Ciliated Cells Are Primary Targets for SARS-CoV-2 Replication in the Early Stage of COVID-19. *J. Clin. Invest.* **2021**, *131*, e148517, doi:10.1172/JCI148517.
21. Bunyavanich, S.; Do, A.; Vicencio, A. Nasal Gene Expression of Angiotensin-Converting Enzyme 2 in Children and Adults. *JAMA* **2020**, *323*, 2427, doi:10.1001/jama.2020.8707.
22. Corbett, K.S.; Edwards, D.; Leist, S.R.; Abiona, O.M.; Boyoglu-Barnum, S.; Gillespie, R.A.; Himansu, S.; Schäfer, A.; Ziwawo, C.T.; DiPiazza, A.T.; et al. *SARS-CoV-2 MRNA Vaccine Development Enabled by Prototype Pathogen Preparedness*; Immunology, 2020;
23. McMahan, K.; Yu, J.; Mercado, N.B.; Loos, C.; Tostanoski, L.H.; Chandrashekar, A.; Liu, J.; Peter, L.; Atyeo, C.; Zhu, A.; et al. Correlates of Protection against SARS-CoV-2 in Rhesus Macaques. *Nature* **2021**, *590*, 630–634, doi:10.1038/s41586-020-03041-6.
24. Zhao, J.; Zhao, J.; Perlman, S. T Cell Responses Are Required for Protection from Clinical Disease and for Virus Clearance in Severe Acute Respiratory Syndrome Coronavirus-Infected Mice. *J. Virol.* **2010**, *84*, 9318–9325, doi:10.1128/JVI.01049-10.
25. Zhuang, Z.; Lai, X.; Sun, J.; Chen, Z.; Zhang, Z.; Dai, J.; Liu, D.; Li, Y.; Li, F.; Wang, Y.; et al. Mapping and Role of T Cell Response in SARS-CoV-2–Infected Mice. *J. Exp. Med.* **2021**, *218*, e20202187, doi:10.1084/jem.20202187.
26. Tan, A.T.; Linster, M.; Tan, C.W.; Le Bert, N.; Chia, W.N.; Kunasegaran, K.; Zhuang, Y.; Tham, C.Y.L.; Chia, A.; Smith, G.J.D.; et al. Early Induction of Functional SARS-CoV-2-Specific T Cells Associates with Rapid Viral Clearance and Mild Disease in COVID-19 Patients. *Cell Rep.* **2021**, *34*, 108728, doi:10.1016/j.celrep.2021.108728.
27. Rydyznski Moderbacher, C.; Ramirez, S.I.; Dan, J.M.; Grifoni, A.; Hastie, K.M.; Weiskopf, D.; Belanger, S.; Abbott, R.K.; Kim, C.; Choi, J.; et al. Antigen-Specific Adaptive

Immunity to SARS-CoV-2 in Acute COVID-19 and Associations with Age and Disease Severity. *Cell* **2020**, *183*, 996-1012.e19, doi:10.1016/j.cell.2020.09.038.
28. Guebre-Xabier, M.; Patel, N.; Tian, J.-H.; Zhou, B.; Maciejewski, S.; Lam, K.; Portnoff, A.D.; Massare, M.J.; Frieman, M.B.; Piedra, P.A.; et al. *NVX-CoV2373 Vaccine Protects Cynomolgus Macaque Upper and Lower Airways against SARS-CoV-2 Challenge*; Immunology, 2020;
29. Li, W.; Li, X.; Zhao, D.; Liu, J.; Wang, L.; Li, M.; Liu, X.; Li, J.; Wu, X.; Li, Y. Heterologous Prime-Boost with AdC68- and MRNA-Based COVID-19 Vaccines Elicit Potent Immune Responses in Mice. *Signal Transduct. Target. Ther.* **2021**, *6*, 419, doi:10.1038/s41392-021-00843-6.
30. Sapkota, B.; Saud, B.; Shrestha, R.; Al-Fahad, D.; Sah, R.; Shrestha, S.; Rodriguez-Morales, A.J. Heterologous Prime–Boost Strategies for COVID-19 Vaccines. *J. Travel Med.* **2021**, taab191, doi:10.1093/jtm/taab191.
31. Shaw, R.H.; Stuart, A.; Greenland, M.; Liu, X.; Nguyen Van-Tam, J.S.; Snape, M.D. Heterologous Prime-Boost COVID-19 Vaccination: Initial Reactogenicity Data. *The Lancet* **2021**, *397*, 2043–2046, doi:10.1016/S0140-6736(21)01115-6.
32. Gorman, M.J.; Patel, N.; Guebre-Xabier, M.; Zhu, A.L.; Atyeo, C.; Pullen, K.M.; Loos, C.; Goez-Gazi, Y.; Carrion, R.; Tian, J.-H.; et al. Fab and Fc Contribute to Maximal Protection against SARS-CoV-2 Following NVX-CoV2373 Subunit Vaccine with Matrix-M Vaccination. *Cell Rep. Med.* **2021**, *2*, 100405, doi:10.1016/j.xcrm.2021.100405.
33. Fischinger, S.; Fallon, J.K.; Michell, A.R.; Broge, T.; Suscovich, T.J.; Streeck, H.; Alter, G. A High-Throughput, Bead-Based, Antigen-Specific Assay to Assess the Ability of Antibodies to Induce Complement Activation. *J. Immunol. Methods* **2019**, *473*, 112630, doi:10.1016/j.jim.2019.07.002.
34. Karsten, C.B.; Mehta, N.; Shin, S.A.; Diefenbach, T.J.; Slein, M.D.; Karpinski, W.; Irvine, E.B.; Broge, T.; Suscovich, T.J.; Alter, G. A Versatile High-Throughput Assay to Characterize Antibody-Mediated Neutrophil Phagocytosis. *J. Immunol. Methods* **2019**, *471*, 46–56, doi:10.1016/j.jim.2019.05.006.
35. Ackerman, M.E.; Moldt, B.; Wyatt, R.T.; Dugast, A.-S.; McAndrew, E.; Tsoukas, S.; Jost, S.; Berger, C.T.; Sciaranghella, G.; Liu, Q.; et al. A Robust, High-Throughput Assay to Determine the Phagocytic Activity of Clinical Antibody Samples. *J. Immunol. Methods* **2011**, *366*, 8–19, doi:10.1016/j.jim.2010.12.016.
36. Brown, E.P.; Licht, A.F.; Dugast, A.-S.; Choi, I.; Bailey-Kellogg, C.; Alter, G.; Ackerman, M.E. High-Throughput, Multiplexed IgG Subclassing of Antigen-Specific Antibodies from Clinical Samples. *J. Immunol. Methods* **2012**, *386*, 117–123, doi:10.1016/j.jim.2012.09.007.
37. Brown, E.P.; Dowell, K.G.; Boesch, A.W.; Normandin, E.; Mahan, A.E.; Chu, T.; Barouch, D.H.; Bailey-Kellogg, C.; Alter, G.; Ackerman, M.E. Multiplexed Fc Array for Evaluation of Antigen-Specific Antibody Effector Profiles. *J. Immunol. Methods* **2017**, *443*, 33–44, doi:10.1016/j.jim.2017.01.010.

Preprints (www.preprints.org) | NOT PEER-REVIEWED | Posted: 7 June 2022 doi:10.20944/preprints202206.0098.v1

Figure 1: Generation of MAPS complexes. (A) Expression and purification via nickel chromatography of the RBD-Rhizavidin fusion protein. (Left) fluorescein detection of biotin-4-fluorescein (B4F), (right) Coomassie stained SDS-PAGE. 1 μg of each sample was loaded with 1X reducing Laemmli buffer, (-)_indicates samples were not heated and (+) indicates samples were heated for 10 minutes at 100°C. **(B)** Schematic diagram of MAPS technology. **(C)** Binding of S-RBD-Rhizavidin to the human ACE2 receptor. **(D)** HPLC-SEC Chromatograms of S_RBD-Rhizavidin shown in purple, pneumococcal polysaccharide type 1 (PnSP1) shown in red, and MAPS complex shown in black, absorbance at 280nm. **(E)** Mass distribution of samples via SEC-MALS, S_RBD-Rhizavidin shown in purple, PnSP1 shown in red, and MAPS complex shown in black. **(F)** Coomassie stained SDS-PAGE of RBD-Rhizavidin fusion protein, PnSP1, and MAPS complexes. ~1 μg of each sample was loaded with 1X reducing Laemmli buffer, samples on the left side of the ladder were not heated (-) and samples to the right of the ladder were heated for 10 minutes at 100°C (+).

Figure 2: Anti-spike (S) IgG and neutralizing antibodies in rabbits. (A) Design of the rabbit in vivo study **(B)** Anti-S IgG levels (ELISA; OD 450 nm) at days 21 and 42 are shown for placebo (white diamonds) and vaccinated animals (black diamonds). **(C)** SARS CoV-2 virus 50% serum neutralizing titers (VNT50) of sera at days 0, 21, and 42 are shown for placebo and vaccinated animals.

Figure 3: Anti-spike (S) IgG and neutralizing antibodies in non-human primates. (A) Design of the NHP in vivo study **(B)** Anti-S IgG levels (ELISA; OD 450 nm) at days 21 (P1) and 42 (P2) are shown for placebo (P) and vaccinated (V) NHP groups. **(C)** IgG1 levels against S, S1, S2,

Preprints (www.preprints.org) | NOT PEER-REVIEWED | Posted: 7 June 2022 doi:10.20944/preprints202206.0098.v1

RBD, N and HA flu at day 42 are shown for placebo and vaccinated NHP groups. **(D)** IgG3 levels against S, S1, S2, RBD, N from SARS CoV-2 virus and HA flu virus at day 42 are shown for placebo and vaccinated NHP groups. **(E)** SARS CoV-2 virus 50% serum neutralizing titers (VNT50) of sera at days 0, 21, 42 and 49 are shown for placebo (white diamonds) and vaccinated NHP groups (black diamonds). I=immunization, C=challenge, E=euthanasia **(F)** IgG levels against S-RBD protein from D614G or B1.1.7 or B1.351 are shown from sera of vaccinated NHP groups (day 42 serum) (black circles) or from sera coming from seroconverted patients (n=6) (white circles).

Figure 4: MAPS vaccine induces FcγR binding and phagocytic activity in NHP. Binding of SARS CoV-2 specific antibodies to FcγR2a **(A)** and FcγR3a **(B)** was determined by Luminex in sera from placebo (P) and vaccinated NHP (V) groups. **(C)** Using the S or the N SARS CoV-2 protein, the ability of SARS-409 CoV-2 S specific antibody Fc to induce antibody-dependent-complement-deposition (ADCD) **(C)**, neutrophil-phagocytosis (ADNP) **(D)**, or cellular-THP1 monocyte-phagocytosis (ADCP) **(E)** was analyzed for placebo and vaccinated NHP groups.

Figure 5: SARS COV-2 MAPS RBD vaccine induces CD4+ and CD8+ T-cell responses. Splenocytes of placebo (P) or vaccinated (V) NHP groups were re-stimulated *ex vivo* with full-length S peptide mix or buffer. $CD4^+$ Th1 cells **(A)**, Th2 cells **(B)**, Th17 **(C)**, $IFN\gamma^+$ $CD8^+$ **(D)** or $TNF\alpha^+$ $CD8^+$ (E) T-cell specific cytokine release by splenocytes collected from NHP 14 days after second immunization with SARS COV-2 MAPS RBD vaccine or saline (placebo) were determined by flow cytometry after ex vivo restimulation. S-peptide specific responses are corrected for background (no peptide).

Preprints (www.preprints.org) | NOT PEER-REVIEWED | Posted: 7 June 2022 doi:10.20944/preprints202206.0098.v1

Figure 6: MAPS-immunized NHPs had significantly lower viral load compared to control animals. Viral shedding was measured daily for 9 days in nasal swabs by either qRT-PCR **(A)** or $TCID_{50}$ **(B)** or in the lung (bronchoalveolar lavage) at day 2, 4 and 7 by either sgRNA RT-PCR **(C)** or $TCID_{50}$ **(D)**.

Preprints (www.preprints.org) | NOT PEER-REVIEWED | Posted: 7 June 2022 doi:10.20944/preprints202206.0098.v1

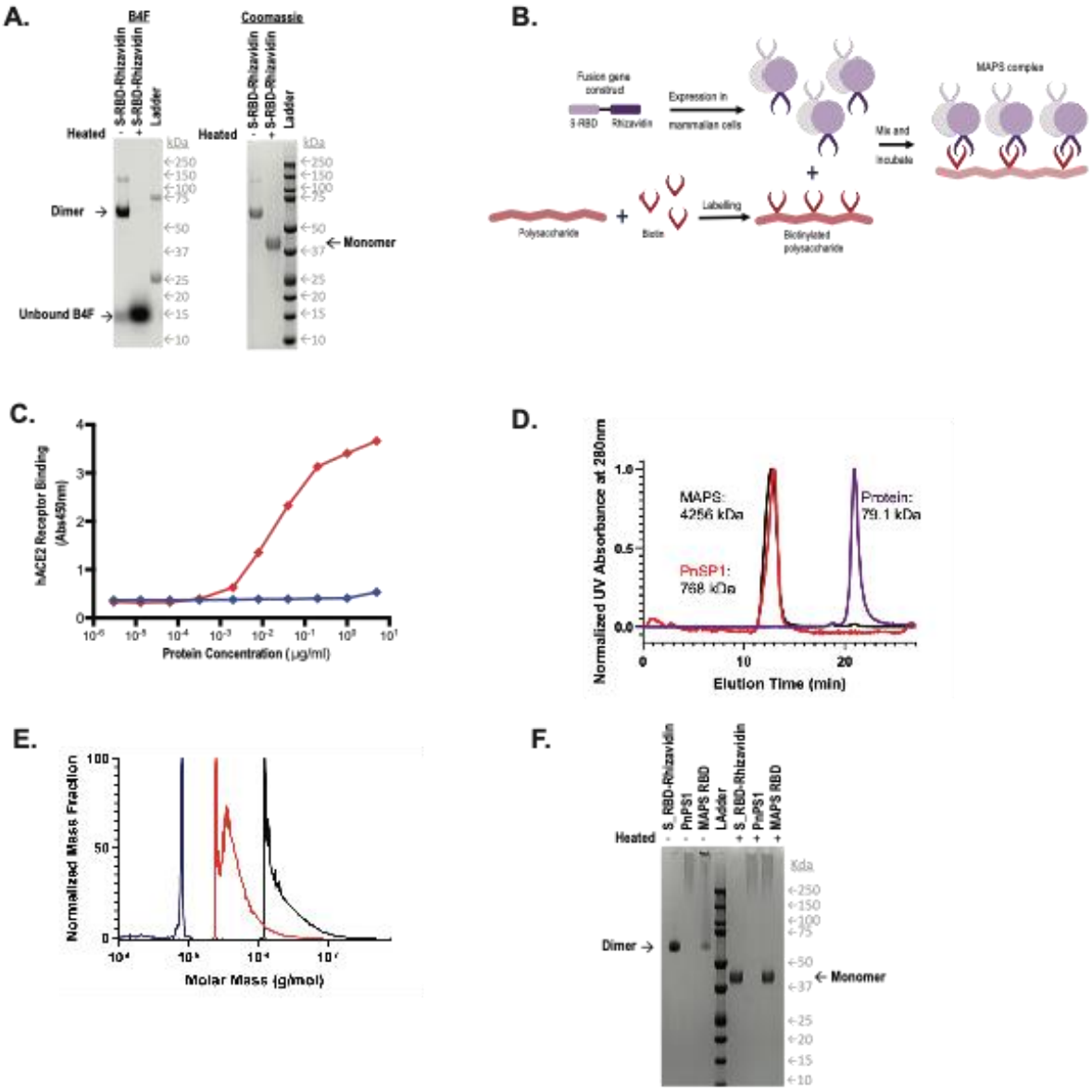

Figure 1

Preprints (www.preprints.org) | NOT PEER-REVIEWED | Posted: 7 June 2022 doi:10.20944/preprints202206.0098.v1

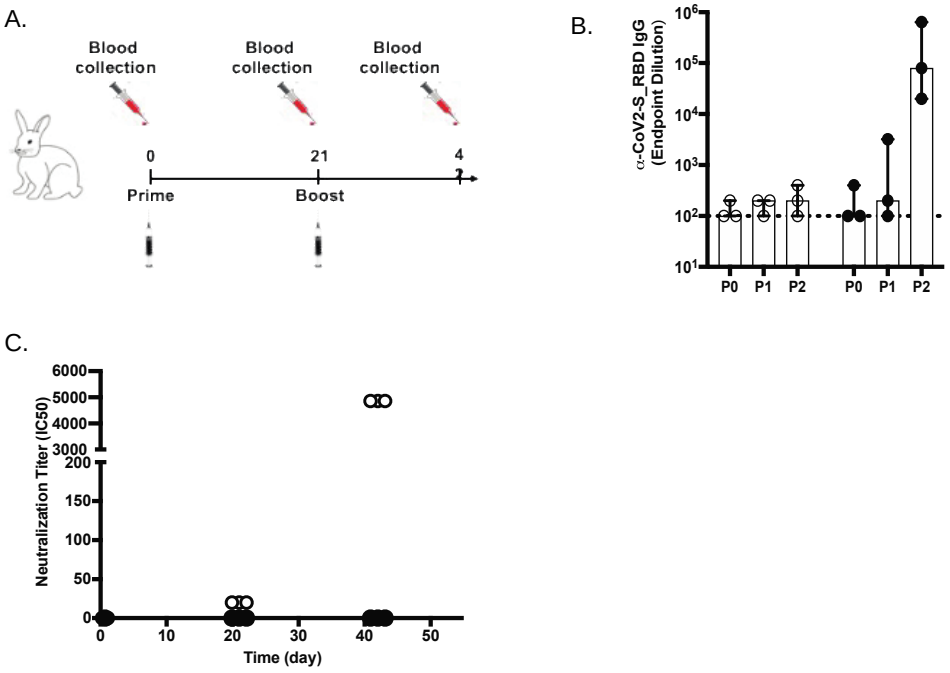

Figure 2

Preprints (www.preprints.org) | NOT PEER-REVIEWED | Posted: 7 June 2022 doi:10.20944/preprints202206.0098.v1

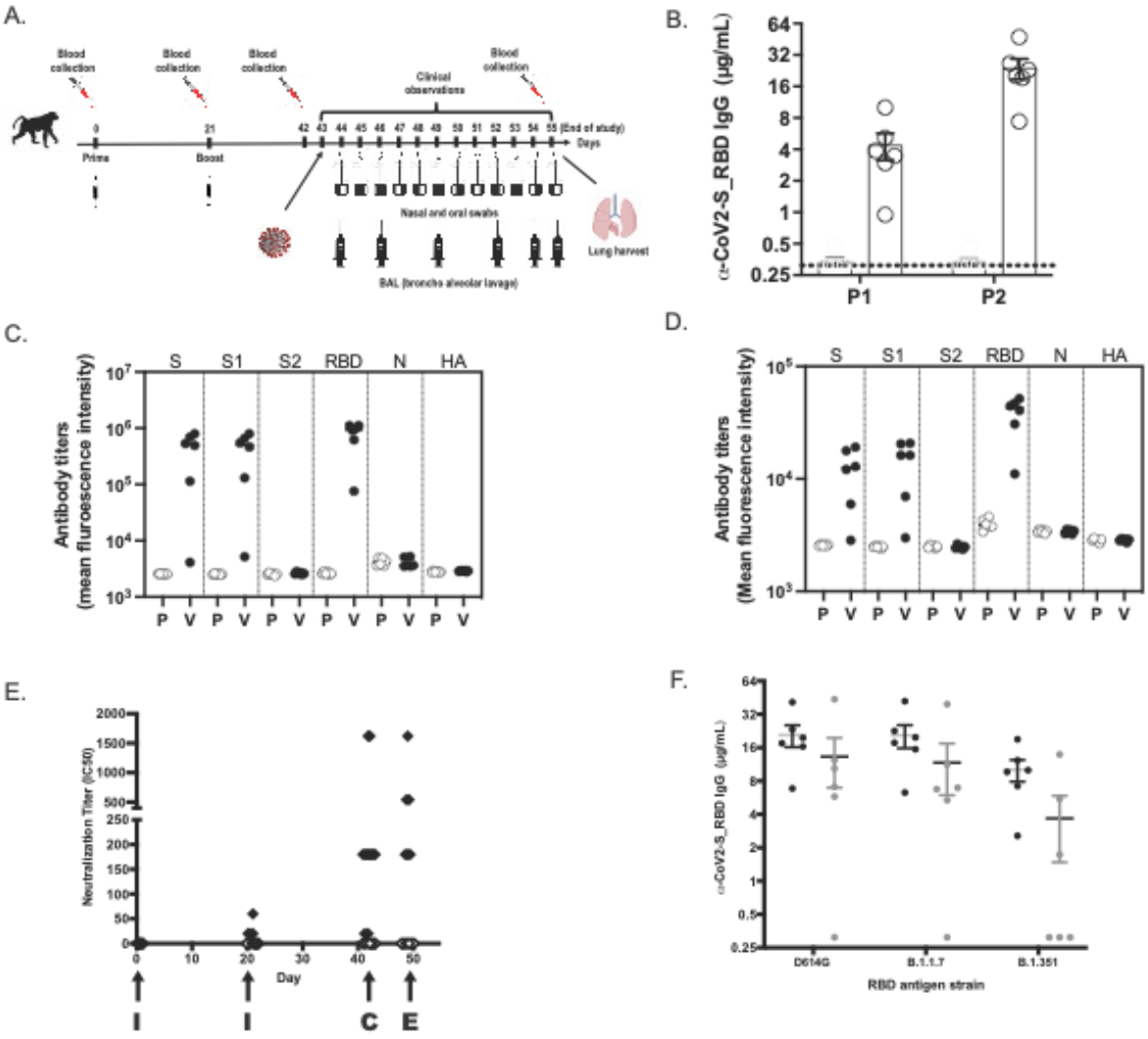

Figure 3

Preprints (www.preprints.org) | NOT PEER-REVIEWED | Posted: 7 June 2022 doi:10.20944/preprints202206.0098.v1

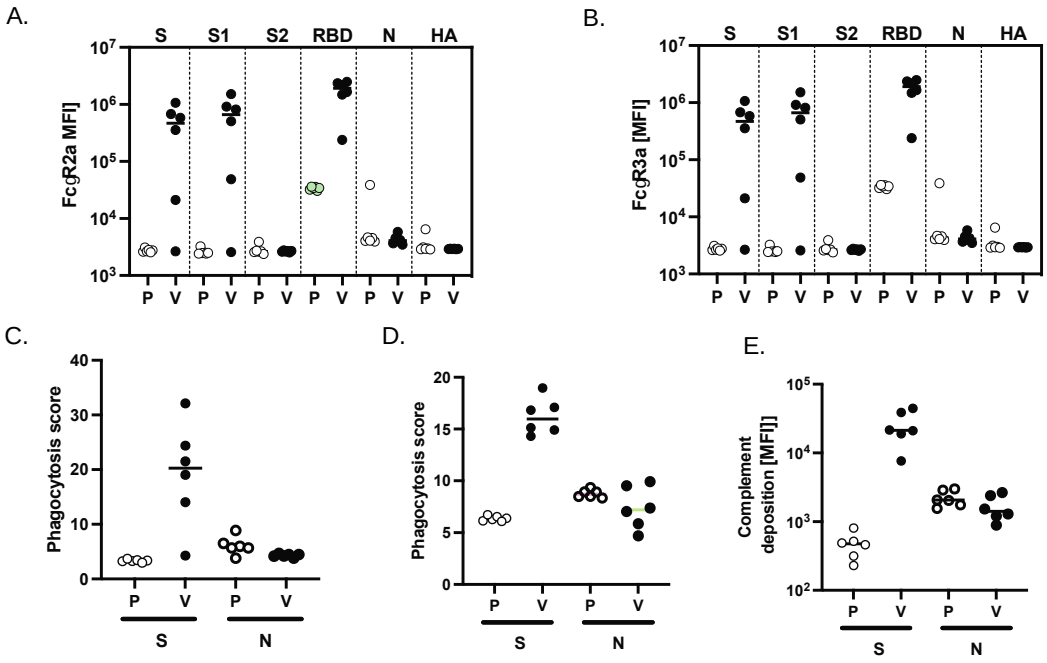

Figure 4

Preprints (www.preprints.org) | NOT PEER-REVIEWED | Posted: 7 June 2022 doi:10.20944/preprints202206.0098.v1

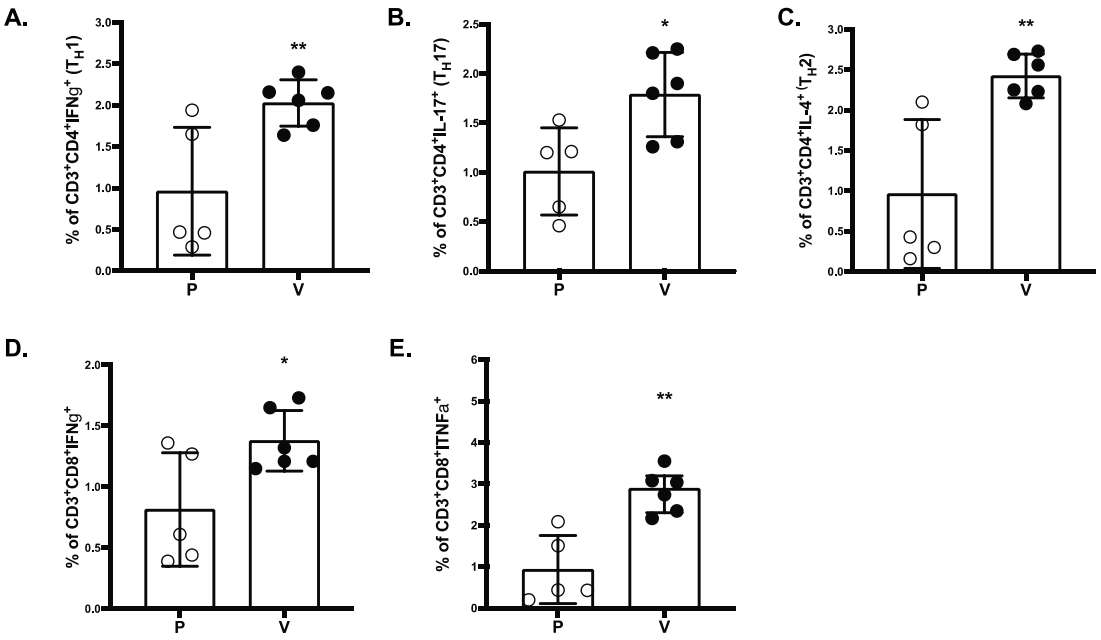

Figure 5

Preprints (www.preprints.org) | NOT PEER-REVIEWED | Posted: 7 June 2022 doi:10.20944/preprints202206.0098.v1

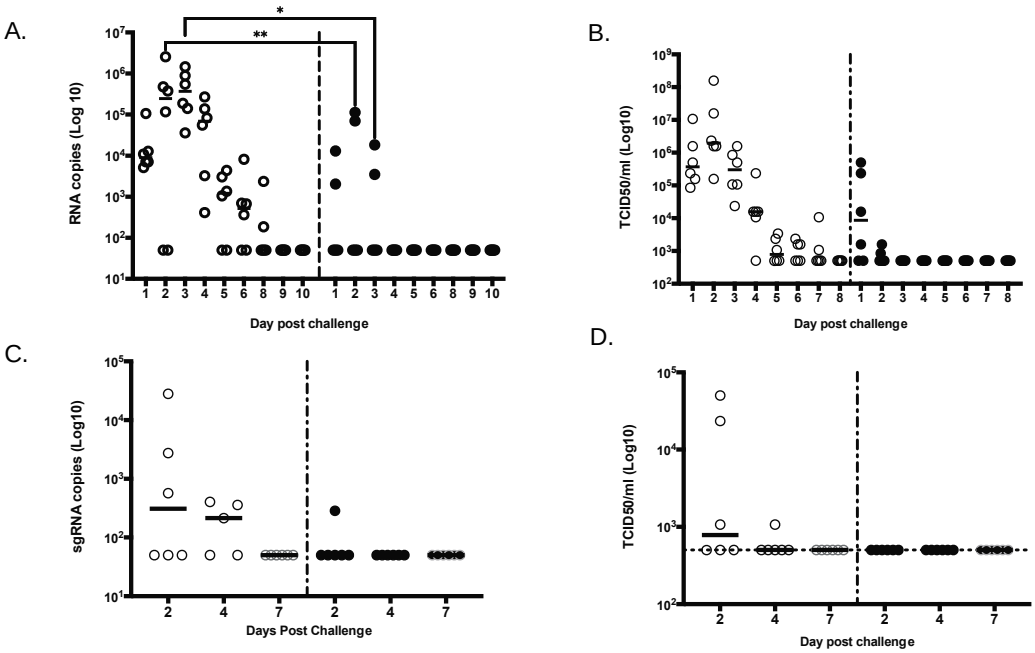

Figure 6